

# *The Functionality of the three-sited Ferroxidase center of E. coli Bacterial Ferritin (EcFtnA)*

Article

Accepted Version

Supporting Info

Bou-Abdallah, F., Yang, H., Awomolo, A., Cooper, B., Woodhall, M.R., Andrews, S.C. ORCID: <https://orcid.org/0000-0003-4295-2686> and Chasteen, N.D. (2014) The Functionality of the three-sited Ferroxidase center of E. coli Bacterial Ferritin (EcFtnA). *Biochemistry*, 53 (3). pp. 483-495. ISSN 0006-2960 doi: <https://doi.org/10.1021/bi401517f> Available at <https://centaur.reading.ac.uk/39349/>

It is advisable to refer to the publisher's version if you intend to cite from the work. See [Guidance on citing](#).

Published version at: <http://pubs.acs.org/doi/abs/10.1021/bi401517f>

To link to this article DOI: <http://dx.doi.org/10.1021/bi401517f>

Publisher: American Chemical Society

All outputs in CentAUR are protected by Intellectual Property Rights law, including copyright law. Copyright and IPR is retained by the creators or other copyright holders. Terms and conditions for use of this material are defined in the [End User Agreement](#).

[www.reading.ac.uk/centaur](http://www.reading.ac.uk/centaur)

**CentAUR**

Central Archive at the University of Reading

Reading's research outputs online

## SUPPORTING INFORMATION

### The Functionality of the Three-Sited Ferroxidase Center of *E. Coli* Bacterial Ferritin (EcFtnA)<sup>\*</sup>

F. Bou-Abdallah<sup>#, §</sup>, H. Yang<sup>#</sup>, A. Awomolo<sup>#</sup>, B. Cooper<sup>#</sup>, M. Woodhall<sup>¶</sup>, S. C. Andrews<sup>¶</sup>,  
and N. D. Chasteen<sup>‡</sup>

<sup>#</sup> Department of Chemistry, State University of New York, Potsdam, NY 13676, USA, <sup>¶</sup> Microbial Biochemistry, School of Animal & Microbial Sciences, University of Reading, Whiteknights, PO Box 228, Reading RG6 6AJ, UK and <sup>‡</sup> Department of Chemistry, University of New Hampshire, Durham, NH 03824, USA.

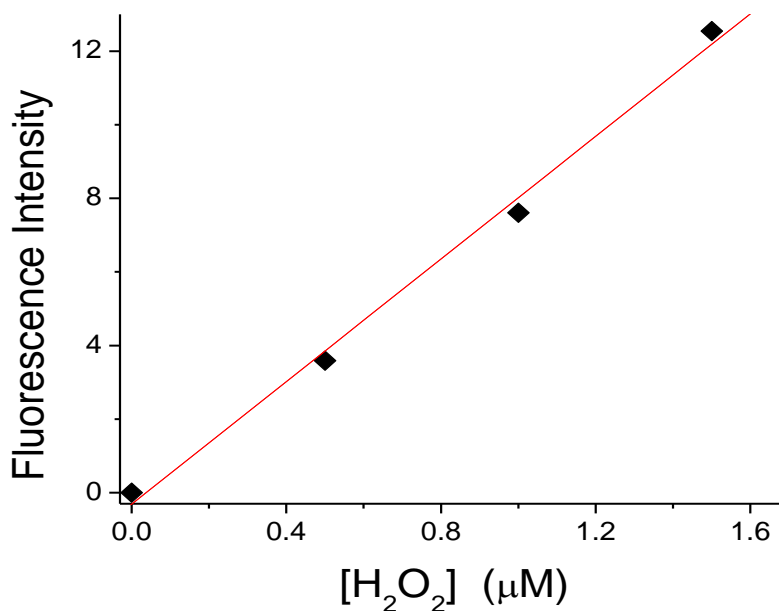


Figure S1: Standard curve for Amplex Red assay.

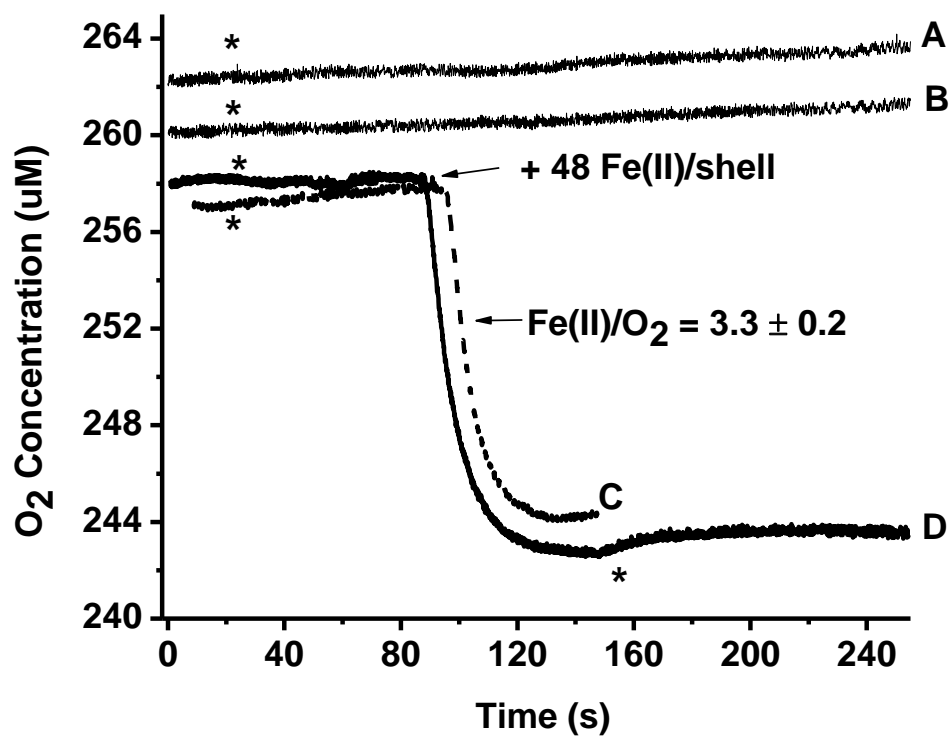


Figure S2: Oxygen consumption curves for (A) ApoEcFtnA (1 uM) in 0.1 M Mops, 50 mM NaCl, pH 7.0 + 1 ul catalase (1300 units); (B) buffer alone + 1 ul catalase; (C) EcFtnA (1 uM) in 0.1 M Mops, 50 mM NaCl, pH 7.0 + 1 ul catalase followed by 48 Fe(II)/shell; (D) EcFtnA (1 uM) in 0.1 M Mops, 50 mM NaCl, pH 7.0 + 48 Fe(II)/shell followed the addition of 1 ul catalase at the end of the oxidation reaction (the star denotes the addition of catalase).

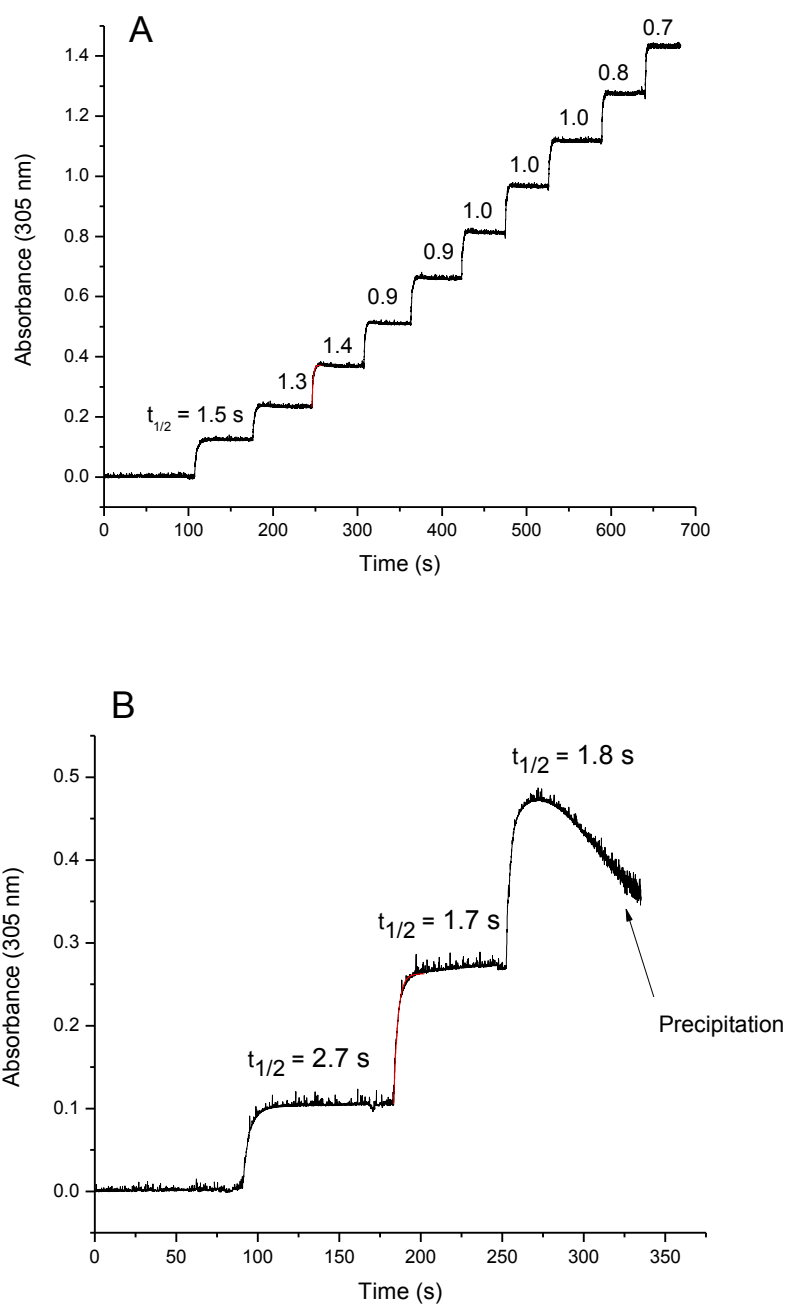
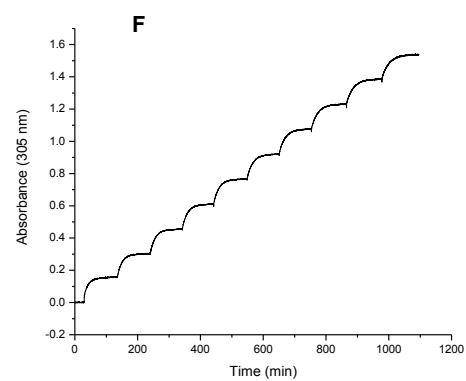
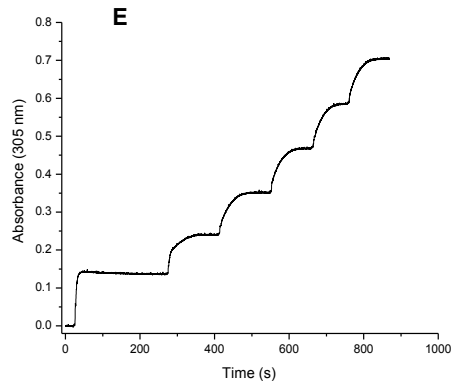
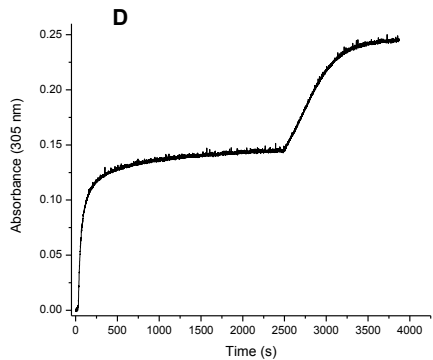
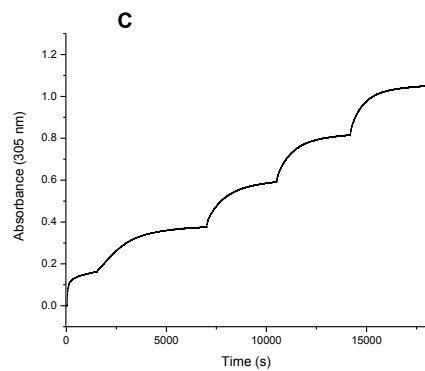
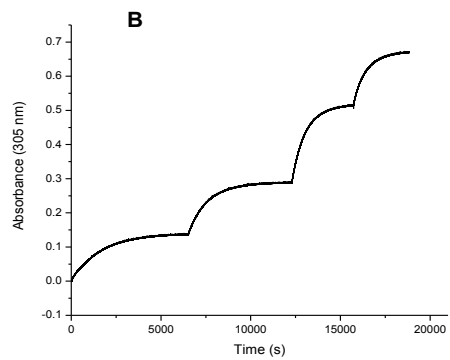
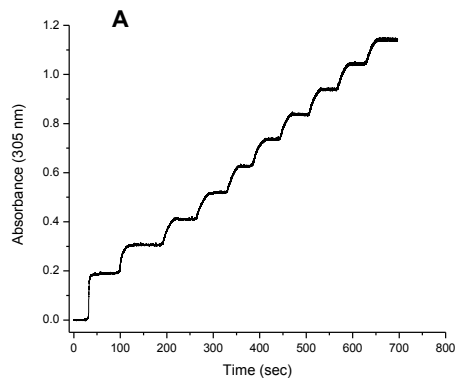


Figure S3: (A) Multiple anaerobic additions of 48 Fe(II)/shell to apoEcFtnA (1  $\mu$ M) in 0.1 M Mops, 0.1 M NaCl, pH 7.00 followed by 24 H<sub>2</sub>O<sub>2</sub>/shell. Half-lives in seconds from single exponential fits are indicated. Fitting errors are  $\pm 0.02$  s. (B) Two anaerobic additions of 500 Fe(II)/shell to apoEcFtnA (0.1  $\mu$ M) in 0.1 M Mops, 0.1 M NaCl, pH 7.00 followed by 250 H<sub>2</sub>O<sub>2</sub>/shell. The third addition of 500 Fe(II)/shell led to protein precipitation. Half-lives from single exponential fits are indicated. Fitting errors are  $\pm 0.03$  s.



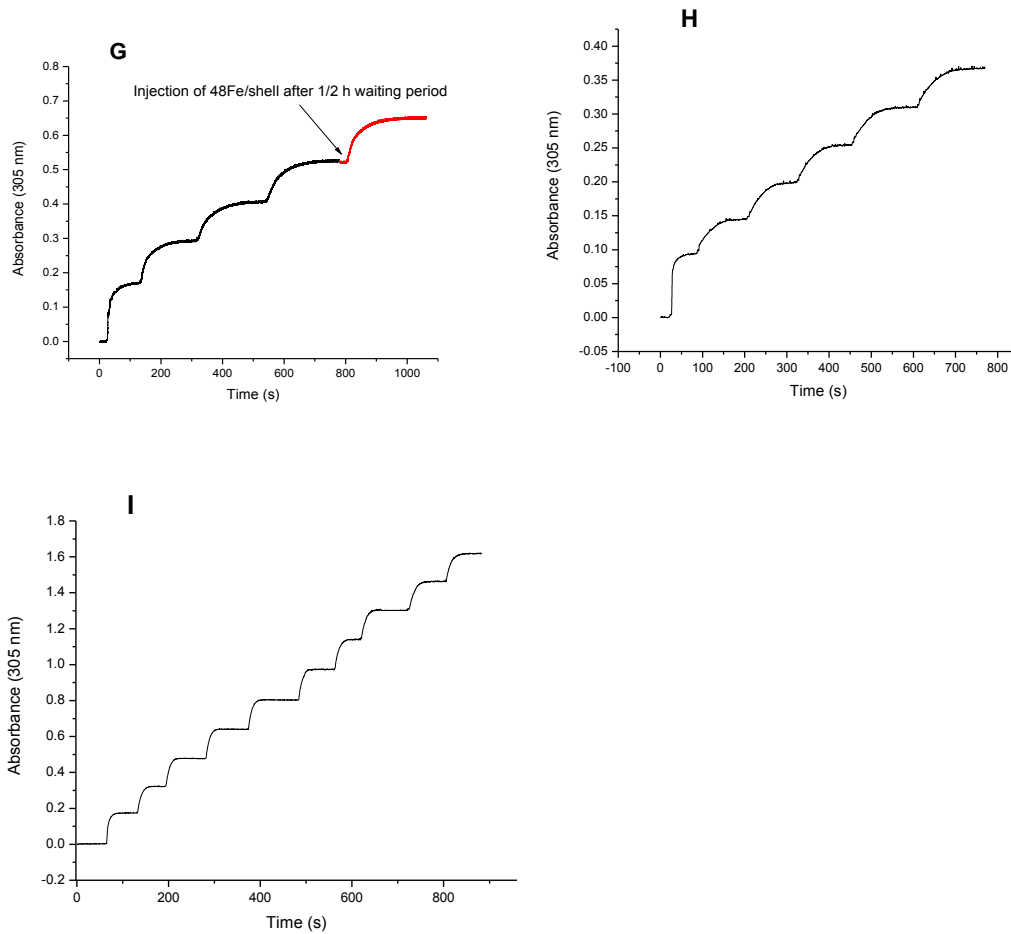


Figure S4: Absorbance-time curve for multiple aerobic additions of  $^{48}\text{Fe(II)}$  per shell to  $1\ \mu\text{M}$  protein solutions (except Y24F at  $0.5\ \mu\text{M}$ ) in  $0.1\ \text{M}$  Mops,  $50\ \text{mM}$  NaCl, pH 7.02. Derived half-lives for oxidation are given in Table 2. (A) Wt EcFTnA, (B) H53A, (C) E17A, (D) E94A, (E) E130A, (F) E 49A, (G) E126A, (H) Y24F, (I) HuHF

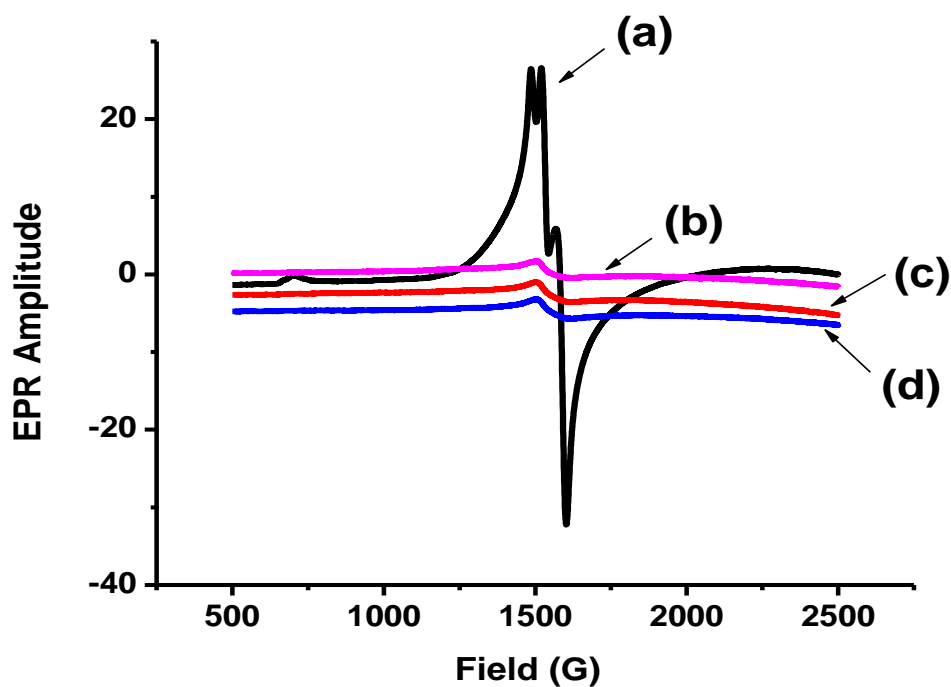


Figure S5: EPR spectra of frozen solutions of (A)  $\text{Fe}^{3+}$ -human transferrin (0.427 mM monoferric C-lobe transferrin) in 20 mM  $\text{NaHCO}_3$ , 50 mM Mops, pH 7.0, (B) EcFtnA + 48 Fe(II) per shell (0.427 mM  $\text{Fe}^{3+}$ ), (C) sample B + another 24 Fe(II)/shell to give a total of 72 Fe(II)/shell (0.64 mM  $\text{Fe}^{3+}$ ), (D) EcFtnA + 72 Fe(II) per shell (0.64 mM  $\text{Fe}^{3+}$ ) added in one shot. Conditions:  $[\text{EcFtnA}] = 8.9 \text{ }\mu\text{M}$  in 0.1 M Mops and 50 mM NaCl, pH 7.0. Sample B was frozen 2 minutes after adding  $\text{Fe}^{2+}$ ; Sample C was frozen 2-3 minutes after thawing sample A and adding 24 more Fe/shell; Sample D was frozen 5 minutes following the one shot addition of 72 Fe(II)/shell.



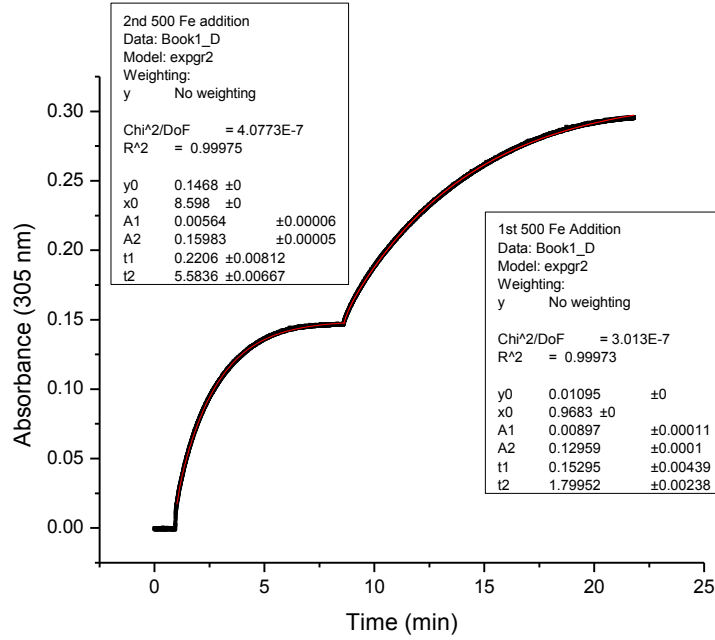


Figure S6: Iron uptake curves for two additions of 500 Fe(II) additions to apoEcFtnA (0.1  $\mu$ M) in 0.1 M Mops, 0.1 M NaCl, pH 7.00. Red lines are fitted curves with fitting parameters given in the boxes. Fitting function

$$y = y_0 + A_1[1 - \exp(-(x_0 - x)/t_1)] + A_2[1 - \exp(-(x_0 - x)/t_2)]$$

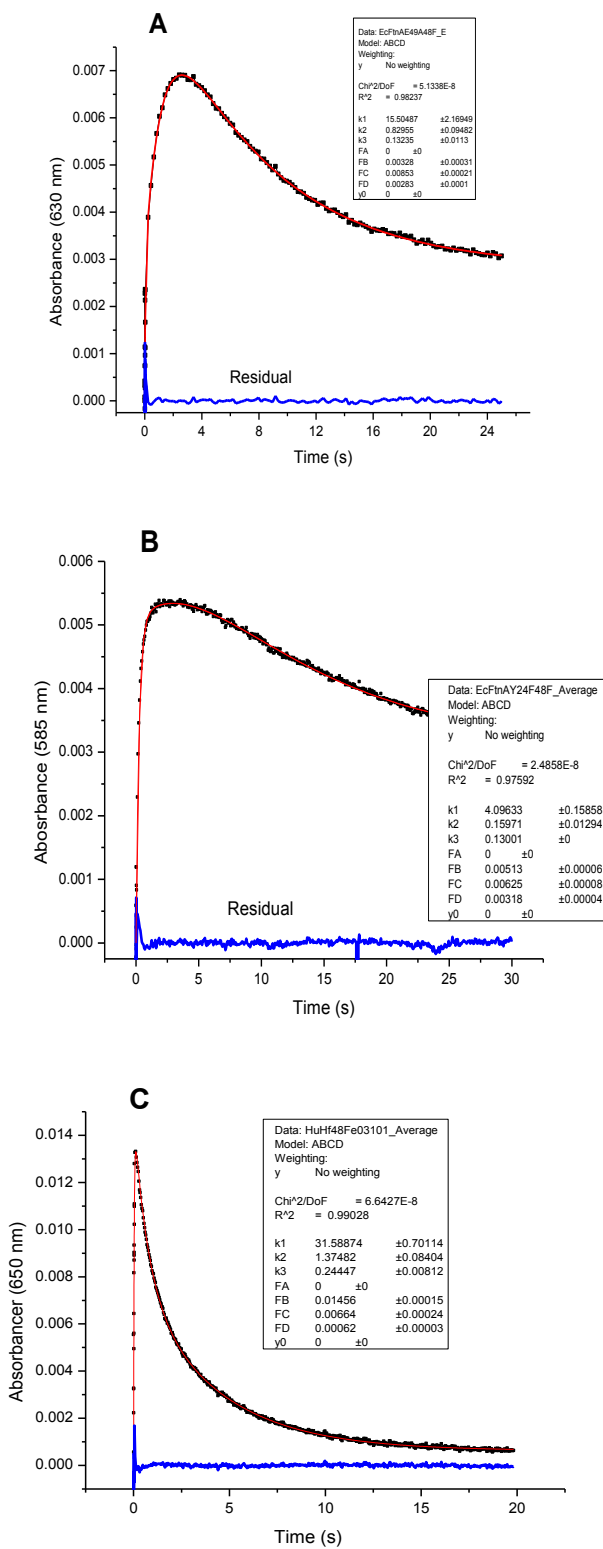


Figure S7: Stopped-flow kinetics curve for peroxo complex formation and decay in (A) E49A, (B) Y24F and (C) HuHF.

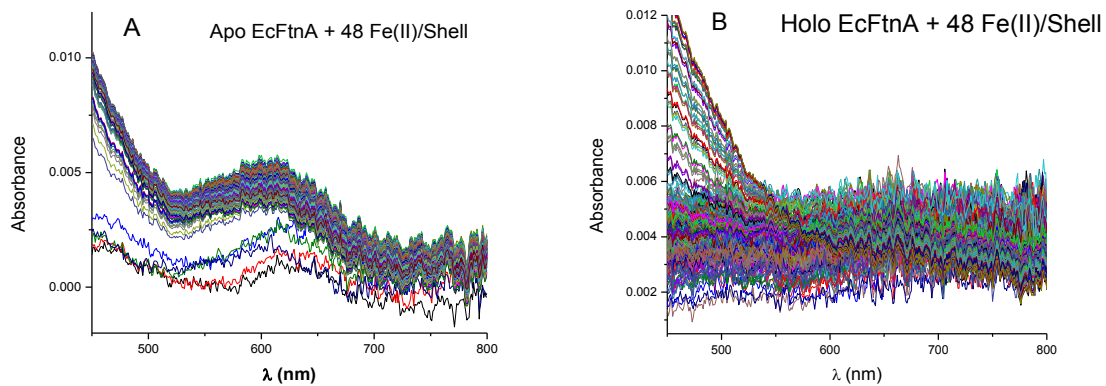


Figure S8: Multiwavelength stopped-flow spectra of (A) ApoEcFtnA (1  $\mu$ M) in 0.1 M + 48 Fe(II)/shell and (B) Holo ferritin (1.5  $\mu$ M) containing 72 Fe(III)/shell + 48 Fe(II)/shell, both in 0.1 M Mops, 0.1 M NaCl, pH 7.0. Spectra scaled to 1  $\mu$ M protein concentration.

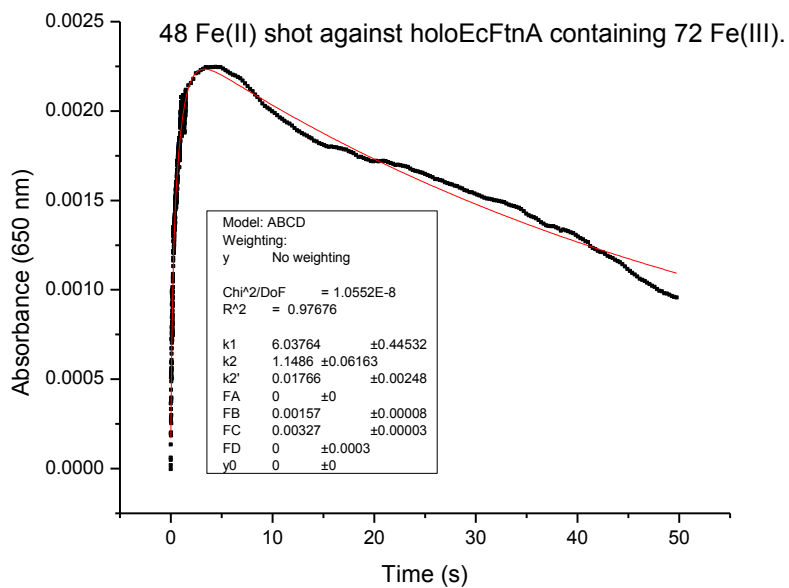


Figure S9: Stopped-flow kinetic curve at 650 nm for weak absorbance in Fig. S7B. Fit is only approximated by a  $A \xrightarrow{k_1} B \xrightarrow{k_2} B' \xrightarrow{k_2'} C$  model.

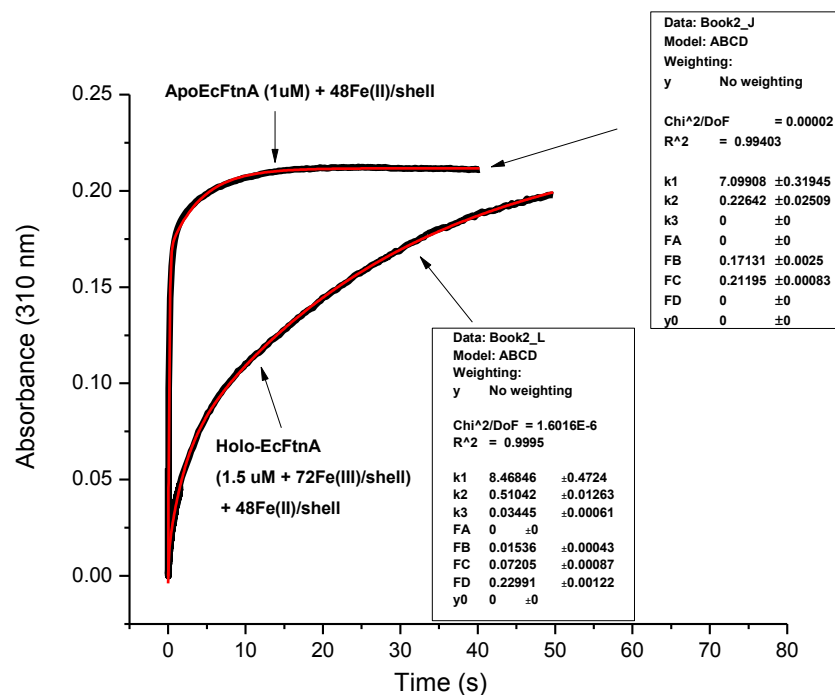


Figure S10: Stopped-flow absorbance-time curve at 310 nm for apoEcFtnA + 48 Fe(II)/shell and Holo EcFtnA + 48 Fe(II)/shell. Curve for HoloEcFtnA has been scaled to 1  $\mu$ M protein concentration. Conditions: 0.1 M Mops, 0.1M NaCl, pH 7.

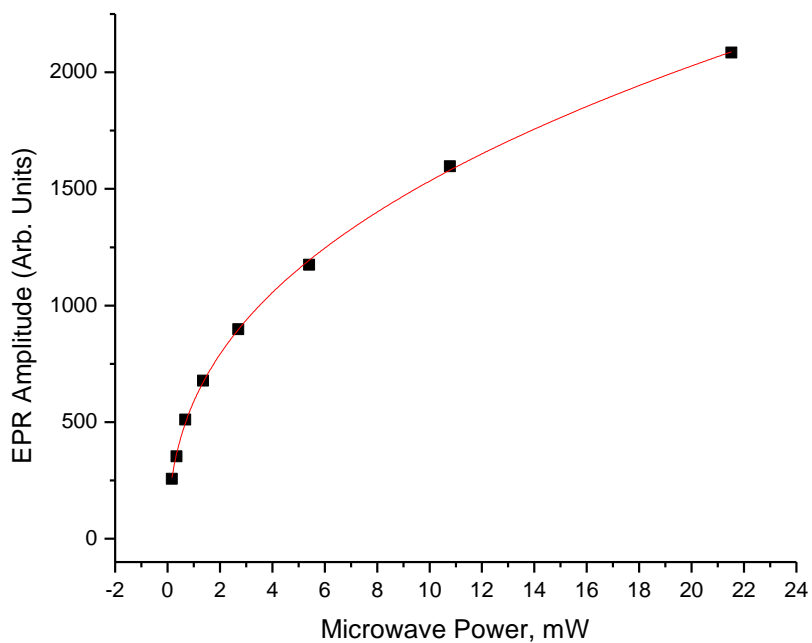
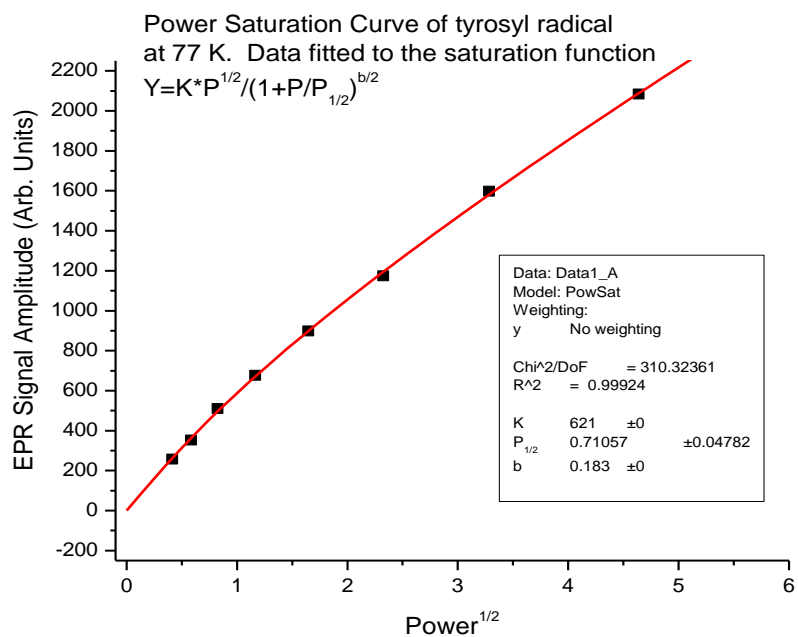


Figure S11: EPR power saturation curves of tyrosine radical signal.